T_c for dilute Bose gases: Beyond leading order in $1/N$

Peter Arnold and Boris Tomášik
Department of Physics, University of Virginia, P.O. Box 400714, Charlottesville, Virginia 22904-4714
(Received 23 May 2000; published 9 November 2000)

Baym, Blaizot, and Zinn-Justin have recently used the large-N approximation to calculate the effect of interactions on the transition temperature of dilute Bose gases. We extend their calculation to next-to-leading order in $1/N$ and find a relatively small correction of -26% to the leading order result. This suggests that the large-N approximation works surprisingly well in this application.

PACS number(s): 03.75.Fi, 11.15.Pg, 64.70.$-$p

I. INTRODUCTION

Second-order phase transitions have universal behavior, associated with long-wavelength fluctuations, for which critical exponents and other universal quantities can often be successfully calculated using renormalization-group techniques. For most such systems, the short distance physics is hopelessly complicated. In contrast, the phase transition of a dilute, interacting Bose gas provides a fascinating example where physics becomes simpler, and perturbative, at (relatively) small distance scales. For this system, it should be possible to marry techniques for treating long-distance critical fluctuations to a perturbative treatment of short-distance physics, and so compute nonuniversal characteristics of the phase transition. A simple example of such a nonuniversal quantity is the phase-transition temperature T_c, and the effect of interactions on T_c has been explored by several authors [1–6], with a wide variety of theoretical results. In particular, the transition temperature has recently been calculated by Baym, Blaizot, and Zinn-Justin [7] in the large-N approximation. For simplicity, they implicitly focus on the case of Bose gases with a single spin state, where the low-energy cross section for atomic collisions can be parametrized by a single scattering length, a. As will be briefly reviewed below, the problem is first reduced to a calculation in a three dimensional O(2) scalar field theory at its critical point. Replacing that by an O(N) theory with $N=2$, they find

$$T_c = T_0\left[1+\frac{8\pi}{3\zeta(3/2)^{4/3}}an^{1/3}[1+O(N^{-1})]+O((an^{1/3})^2)\right] \tag{1.1}$$

in the dilute limit, where n is the number density and T_0 is the transition temperature of a noninteracting Bose gas,

$$T_0 = \frac{2\pi\hbar^2}{k_B m}\left(\frac{n}{\zeta(3/2)}\right)^{2/3}. \tag{1.2}$$

For simplicity, we consider a uniform Bose gas, where n is fixed. Alternatively, in an arbitrarily wide harmonic trap, n should be interpreted as the actual density at the center of the trap at the transition temperature.

Baym *et al.*'s result (1.1) of $\Delta T_c/T_0 \equiv (T_c - T_0)/T_0 \simeq 2.33an^{1/3}$ is in good agreement with recent numerical simulations [6] that give $\Delta T_c/T_0 \approx (2.2\pm 0.2)an^{1/3}$. The result is surprising because it seems to work much better than the large-N expansion of critical exponents. For example, for O(N) theory, the susceptibility critical exponent γ is [9][1]

$$\gamma = 2-\frac{24}{N\pi^2}+\frac{64}{N^2\pi^4}\left(\frac{44}{9}-\pi^2\right)+O(N^{-3})$$
$$=2-1.216\left(\frac{2}{N}\right)-0.818\left(\frac{2}{N}\right)^2+O(N^{-3}). \tag{1.3}$$

This is not a marvelous expansion for $N=2$, for which the actual value is $\gamma \simeq 1.32$.

In this paper, we calculate the $O(N^{-1})$ relative correction to Eq. (1.1). We find

$$T_c = T_0\left[1+\frac{8\pi}{3\zeta(3/2)^{4/3}}an^{1/3}\left[1-\frac{0.527\,198}{N}+O(N^{-2})\right] + O((an^{1/3})^2)\right]. \tag{1.4}$$

Setting $N=2$, this is only a 26% correction to the leading large-N result for $\Delta T_c/T_0$. We now have $\Delta T_c/T_0 \simeq 1.71an^{1/3}$. Though this does not agree as well with the quoted simulation result, the moderately small size of the correction supports the proposition that the large-N expansion works surprisingly well for T_c.

---

[1]For Bose gases, a more physical example of a critical exponent is $\nu = 1-0.540(2/N)-0.470(2/N)^2+O(N^{-3})$, whose actual value is $\nu \simeq 0.67$ for $N=2$. The fact that O(2) critical exponents should be identified with Bose-gas exponents is not completely trivial. A uniform, nonrelativistic Bose gas is a constrained system: the particle density n is fixed. This constraint causes the critical exponents $\tilde{x} = (\tilde{\alpha},\tilde{\beta},\tilde{\gamma},\tilde{\nu})$ of the actual system to be related [10] to the standard exponents $x=(\alpha,\beta,\gamma,\nu)$ of the field theory by (i) $\tilde{\alpha}=-\alpha/(1-\alpha)$, and $\tilde{x}=x/(1-\alpha)$ for the others, if $\alpha>0$, or (ii) $\tilde{x}=x$ if $\alpha<0$. The actual value of α for the O(2) model is believed to be -0.007 ± 0.006 [11]. If negative, there is no difference between the exponents; if positive, there is in principle a very tiny difference. This relation explains, by the way, the difference between mean-field theory exponents for the O(2) model (e.g., $\alpha=\frac{1}{2}$) and the exponents of a noninteracting Bose gas (e.g., $\tilde{\alpha}=-1$).

In the remainder of this Introduction, we review the long-distance O(2) effective theory for Bose condensation and then review the arguments of [5,7] about how to calculate $\Delta T_c/T_c$. In Sec. II, we review the leading-order calculation in large N as done in [7]. In Sec. III, we go on to calculate the next order in $1/N$. An Appendix explains how to calculate some of the basic three-dimensional integrals that appear at that order.

But first, we should mention some experimental data on the ^{4}He-Vycor system [8]. As alluded to earlier, there have been several different theoretical results and simulation results for $\Delta T_c/T_0$, obtained by various methods (e.g., [1–4]), giving a large range of values for the coefficient of $an^{1/3}$ in $\Delta T_c/T_0$. Superficially, the ^{4}He-Vycor data seem to fit well an early theoretical estimate of Stoof [3], which is $\Delta T_c/T_0 \simeq (16\pi/3)\zeta(3/2)^{-4/3}an^{1/3} \simeq 4.66 an^{1/3}$ (exactly twice the leading-order large-N result). However, the detailed interpretation of this data is unclear. In that experiment, the helium atoms are confined to an interconnected network of channels in the porous Vycor glass, and, for the low-density data that appear to fit Stoof, the interparticle spacing is the same order of magnitude as the widths of the channels. Reference [8] simply assumes that the system can be modeled by a free Bose gas with (i) an effective mass for the atoms that is extracted experimentally, but (ii) the same scattering length as for bulk helium, which is moreover taken from theoretical modeling. Because of these assumptions, the apparent agreement with the early work of Stoof should be treated with caution.

A. Review of effective theory

The basic assumption throughout will be that the average separation $n^{-1/3}$ of atoms is large compared to the scattering length a. This can also be expressed as $\lambda(T_0) \gg a$, where λ is the thermal wavelength

$$\lambda(T) = \left(\frac{2\pi\hbar^2}{mk_BT}\right)^{1/2}. \tag{1.5}$$

It is well known that, at distance scales large compared to the scattering length a, an appropriate effective theory for a dilute Bose gas is the second-quantized Schrödinger equation, together with a chemical potential μ that couples to particle number density $\psi^*\psi$, and a $|\psi|^4$ contact interaction that reproduces low-energy scattering. The corresponding Lagrangian is

$$\mathcal{L} = \psi^*\left(-i\hbar\partial_t - \frac{\hbar^2}{2m}\nabla^2 - \mu\right)\psi + \frac{2\pi\hbar^2 a}{m}(\psi^*\psi)^2. \tag{1.6}$$

In this context, the corresponding mean-field equation of motion is called the Gross-Pitaevskii equation. (For a review, see [12].) As with any effective theory, there are corrections represented by higher-dimensional, irrelevant interactions (in the sense of the renormalization group),[2] such as $(\psi^*\psi)^3$ and $\psi^*\nabla^4\psi$. However, higher and higher dimension operators are parametrically less and less important if the distance scales of interest are large compared to the characteristic scales (a) of the atomic interactions. The $(\psi^*\psi)^2$ term in the Lagrangian (1.6) is in fact the lowest-dimension irrelevant interaction, and it is adequate for computing the leading-order effects of interactions in the diluteness expansion. (For a discussion of analyzing corrections in this language, see Ref. [13], which extended earlier work on corrections by Refs. [14]. A similar discussion for Fermi gases may be found in Ref. [15].)

Now treat the system at finite temperature using the imaginary time formalism. The field can then be decomposed into frequency modes with Matsubara frequencies $\omega_n = 2\pi n k_B T/\hbar$. At sufficiently large distance scales ($\gg\lambda$), and small chemical potential ($|\mu| \ll k_BT$), the $-(\hbar^2/2m)\nabla^2 - \mu$ terms in Eq. (1.6) become small compared to the $O(\hbar\omega_n)$ time derivative term, provided $n \neq 0$. The nonzero Matsubara frequency modes then decouple from the dynamics, leaving behind an effective theory of only the zero-frequency modes ψ_0. Roughly,

$$\frac{1}{\hbar}\int_0^{\hbar\beta} dt \int d^3x\,\mathcal{L} \to \beta\int d^3x\left[\psi_0^*\left(-\frac{\hbar^2}{2m}\nabla^2 - \mu\right)\psi_0 + \frac{2\pi\hbar^2 a}{m}(\psi_0^*\psi_0)^2\right] \tag{1.7}$$

with $\beta = 1/k_BT$. In detail, the parameters of (1.7) are renormalized by coupling to the nonzero modes, and there are again corrections in the form of irrelevant (and even marginal) interactions. However, these effects are all suppressed in the dilute limit[3] and do not affect the computation of $\Delta T_c/T_0$ at leading order in $an^{1/3}$.

It is then convenient to write $\psi_0 = \hbar^{-1}(mk_BT)^{1/2}(\phi_1 + i\phi_2)$ so that the effective action $S = H/T$ becomes a conventionally normalized O(2) field theory:

---

[2]At short distances, the ∂_t and ∇^2 terms of the action $\int dt d^3x \mathcal{L}$ determine that times scales as (length)^2 and the scaling dimension of ψ is (length)$^{-3/2}$.

[3]For the three-dimensional effective theory (1.7), the short-distance scaling dimension of ψ_0 is (length)$^{-1/2}$, the $(\psi_0^*\psi_0)^2$ interaction is relevant, and a $(\psi_0^*\psi_0)^3$ interaction would be marginal. Even though marginal, this last interaction can be ignored at the order of interest in the diluteness expansion because it has a small coefficient. For example, consider the term that would arise directly from the presence of a correction $g_3(\psi^*\psi)^3$ to the original Lagrangian (1.6). That would lead to a $g_3(\psi_0^*\psi_0)^3$ term in (1.7) which, after rescaling, would become a term proportional to $(mg_3/\hbar^2\lambda^4)(\phi^2)^3$ in Eq. (1.8). Since $\lambda \simeq \lambda(T_0) \propto n^{-1/3}$ at the transition, the coefficient of this term is high order in the diluteness expansion in $n^{1/3}$. Similarly, an effective $(\psi_0^*\psi_0)^3$ term arising from the four-point interactions $(\psi^*\psi)^2$ and from integrating out physics at the scale λ (due, for example, to nonzero Matsubara modes) would give rise to a $(\phi^2)^3$ term in Eq. (1.8) with coefficient proportional to $u^3\lambda^3 \propto \lambda^{-3}$.

$$S=\int d^3x\left[\frac{1}{2}|\nabla\phi|^2+\frac{1}{2}r\phi^2+\frac{u}{4!}(\phi^2)^2\right], \tag{1.8}$$

where ϕ is understood to be a two-component real vector (ϕ_1,ϕ_2) and

$$r=-\frac{2m\mu}{\hbar^2},\quad u=\frac{96\pi^2 a}{\lambda^2}. \tag{1.9}$$

B. Review of $\Delta T_c/T_0$

Our effective theory depends on two as yet undetermined parameters—r and u, or equivalently μ and T. One constraint comes from fixing particle number density n:

$$n=\langle\psi^*\psi\rangle=\frac{mk_BT}{\hbar^2}\langle\phi^2\rangle. \tag{1.10a}$$

At the critical temperature, the system will have infinite correlation length. It will also have an infinite susceptibility χ, which we use as our second constraint:

$$\chi^{-1}=r+\Pi(0)=0, \tag{1.10b}$$

where $\Pi(p)$ is the proper self-energy of the ϕ field. The two equations (1.10) determine the two unknowns r and u, and hence T_c. As noted by Baym *et al.*, the density equation (1.10a) can be rewritten as

$$\frac{\hbar^2 n}{mk_BT}=\int_{\mathbf{p}}\frac{1}{p^2+r+\Pi(p)}=\int_{\mathbf{p}}\frac{1}{p^2+[\Pi(p)-\Pi(0)]}, \tag{1.11}$$

where the last equality uses Eq. (1.10b). Throughout this paper, we will use the notational shorthand

$$\int_{\mathbf{p}}\equiv\int\frac{d^3p}{(2\pi)^3} \tag{1.12}$$

for momentum integrals. (Technically, p is a wave number rather than a momentum, but we will use conventional $\hbar=1$ nomenclature, even though we have not set $\hbar$ to 1.)

Expression (1.11) for the density is ultraviolet (UV) divergent and so receives contributions from short-distance scales where the effective theory breaks down. This could be handled by appropriately regulating the effective theory and then perturbatively correcting the UV contribution. As pointed out by Baym *et al.*, it is simpler instead to consider the difference n-$n_0(T)$, where $n_0(T)$ is the same expression in the absence of interactions (i.e., with Π set to zero):

$$\frac{\hbar^2[n-n_0(T)]}{mk_BT}=\int_{\mathbf{p}}\left[\frac{1}{p^2+r+\Pi(p)}-\frac{1}{p^2}\right]=\int_{\mathbf{p}}\left[\frac{1}{p^2+[\Pi(p)-\Pi(0)]}-\frac{1}{p^2}\right]. \tag{1.13}$$

$n_0(T)$ represents the density a *noninteracting* Bose gas has if its transition temperature is T. It is given by inverting Eq. (1.2):

$$n_0(T)=\frac{\zeta(3/2)}{\lambda^3(T)}. \tag{1.14}$$

This formula cannot be derived directly in the effective theory (1.8), but the difference n-n_0 in Eq. (1.13) is insensitive to the UV and so can be.

The above constraints are entirely adequate to systematically determine ΔT_c in the large-N expansion, but there is a convenient way to simplify the bookkeeping a bit. Baym *et al.* give a simple argument that, to leading order in the density expansion,

$$\frac{\Delta T_c}{T_0}\simeq-\frac{2}{3}\frac{[n-n_0(T_c)]}{n}, \tag{1.15}$$

where the factor of 2/3 in Eq. (1.13) arises from the relation $T_0\propto n_0^{2/3}$. Combining Eq. (1.15) with Eq. (1.13), we can summarize as

$$\frac{\Delta T_c}{T_0}\simeq-\frac{2mk_BT_0}{3\hbar^2 n}\int_{\mathbf{p}}\left[\frac{1}{p^2+r+\Pi(p)}-\frac{1}{p^2}\right]=-\frac{2mk_BT_0}{3\hbar^2 n}\int_{\mathbf{p}}\left[\frac{1}{p^2+[\Pi(p)-\Pi(0)]}-\frac{1}{p^2}\right] \tag{1.16}$$

to leading order in $an^{1/3}$. It is also useful to rephrase this, again in terms of the fields ϕ of the effective theory, as

$$\frac{\Delta T_c}{T_0}\simeq-\frac{2mk_BT_0}{3\hbar^2 n}\Delta\langle\phi^2\rangle, \tag{1.17}$$

where

$$\Delta\langle\phi^2\rangle\equiv\langle\phi^2\rangle-\langle\phi^2\rangle_{\Pi\to 0}. \tag{1.18}$$

Note that the problem of calculating $\Delta\langle\phi^2\rangle$ from the action (1.8), subject to the constraint (1.10b), has only one dimensionful scale in it: u. The length scale of this problem, which will be the length scale of the physics that determines $\Delta T_c/T_0$, is therefore

$$u^{-1}\sim\frac{\lambda^2}{a} \tag{1.19}$$

by dimensional analysis. In the dilute limit $\lambda(T_c)\gg a$, this length scale is large compared to λ, which justifies use of the O(2) effective theory (1.8).

II. REVIEW OF LEADING ORDER IN 1/*N*

We now review the leading large-N calculation of $\langle\phi^2\rangle-\langle\phi^2\rangle_{\Pi\to 0}$, and hence of $\Delta T_c/T_0$, by Baym *et al.* The details of our calculation are slightly different from theirs, and

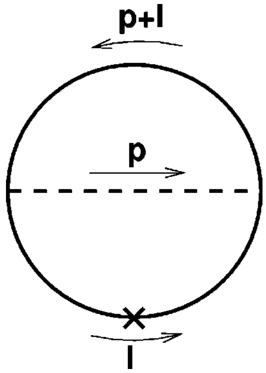

FIG. 1. Diagrams contributing to $\Delta\langle\phi^2\rangle$ at leading order in $1/N$.

we will introduce techniques needed to proceed to higher order. We start with the standard large-N generalization of the O(2) scalar field theory (1.8) to an O(N) scalar theory: replace ϕ by an N-component vector and treat Nu as fixed in the $N\to\infty$ limit. The reader should keep in mind that u is therefore order $1/N$. Standard N power counting of Feynman diagrams consists of a power of $u\sim 1/N$ for each four-point vertex and a power of N for each flavor trace.

The set of diagrams that determine $\Delta\langle\phi^2\rangle$ at leading order in $1/N$ is depicted in Fig. 1, where the dashed line denotes bubble chains, as shown in Fig. 2. (For comparison, the diagram for $\langle\phi^2\rangle_{\Pi\to 0}$ is shown in Fig. 3.) The cross denotes an insertion of the operator ϕ^2, whose expectation we are computing. There is a simple way to summarize the effect on diagrammatic perturbation theory of the $r\phi^2$ term in the action (1.8) and the constraint (1.10b) that $r=-\Pi(0)$.

Rule 1. Use massless (gapless) scalar propagators $1/p^2$ when evaluating diagrams, ignoring the $r\phi^2$ term in the action. But whenever there is a one-particle irreducible subdiagram X that represents a contribution to the ϕ proper self-energy $\Pi(p)$, then[4] replace $X(p)$ by $X(p)-X(0)$.

We note for later reference that, for the purpose of this rule, a diagram that is cut in two pieces only by cutting a single internal *dashed* line is still one-particle irreducible, because cutting the bubble chain represented by a dashed line corresponds to cutting two ϕ lines (Fig. 2).

The bubble chain sum shown in Fig. 2 is given by

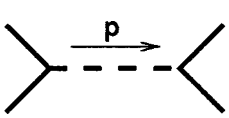

$$= -N^{-1}F_p, \tag{2.1}$$

where

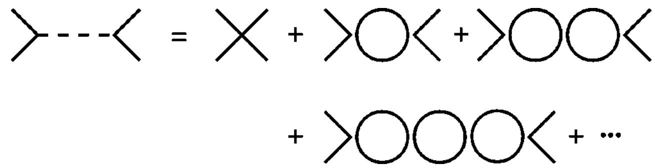

FIG. 2. Bubble chains. Unbroken lines denote flavor index contractions.

$$F_p \equiv \frac{1}{\frac{3}{Nu}+\tilde{\Sigma}_0(p)} \tag{2.2a}$$

and $\tilde{\Sigma}_0(p)$ represents the basic massless bubble integral (not summed over flavors),

$$\tilde{\Sigma}_0(p) \equiv \frac{1}{2}\int_{\mathbf{l}} \frac{1}{l^2|\mathbf{l}+\mathbf{p}|^2}. \tag{2.2b}$$

In $d=3$ dimensions,

$$\tilde{\Sigma}_0(p) = \frac{1}{16p}. \tag{2.3}$$

Putting everything together, the diagram of Fig. 1 gives

$$\Delta\langle\phi^2\rangle = -\int_{\mathbf{lp}} \frac{F_p}{l^4}\left[\frac{1}{|\mathbf{l}+\mathbf{p}|^2}-\frac{1}{p^2}\right]+O(N^{-1}). \tag{2.4}$$

As pointed out by Baym *et al.* in [7], the above integral is not absolutely convergent in three dimensions, and one must be careful to consistently regulate the theory before proceeding. Integrals that are not absolutely convergent are at best ambiguous—they depend on the order one chooses to do the integrations. For example, if one evaluates Eq. (2.4) directly in three dimensions, doing the angular integrations first, then the l integration, and then the p integration, the result is zero. This is not in fact the correct answer. We will discuss this issue in some detail in order to justify the correctness of our procedure for later evaluating higher-order diagrams.

Baym *et al.*'s preferred method for the leading-order calculation is to use dimensional regularization and evaluate everything in $d=3-\epsilon$ dimensions. This is difficult at next order in $1/N$: the loop integrals we shall encounter are sufficiently complicated that evaluation in $d=3-\epsilon$ dimensions

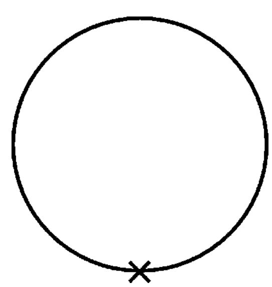

FIG. 3. Diagram representing the noninteracting result $\langle\phi^2\rangle_{\Pi\to 0}$.

[4]This rule is unambiguous for calculating expectations such as $\langle\phi^2\rangle$. It is potentially ambiguous for calculating the free energy—for example, a diagram like Fig. 1 but without the cross on it. In that case, it is ambiguous which subdiagrams would be considered self-energy insertions. A systematic way to treat the perturbation theory in all cases is to treat the $r\phi^2$ term in the action as a perturbation, include it in Feynman diagrams as a two-point vertex, and then set $r=-\Pi(0)$ order by order in perturbation theory.

seems hard. Our strategy will be instead always to reduce diagrams to well-defined three-dimensional integrals, which are simpler to evaluate. We imagine starting with some consistent regularization scheme, such as dimensional regularization, and will now discuss how to manipulate the integrals so that they will be absolutely convergent if we set $d=3$. We assume in what follows that the UV regulator respects parity and is invariant under shifts $\mathbf{p}\to\mathbf{p}+\mathbf{k}$ of loop momenta $\mathbf{p}$.

Let us look at the divergences that cause absolute convergence of the integral (2.4) to fail in three dimensions. A simple one to correct is the behavior for $\mathbf{l}$ fixed and $p\to\infty$. The large p piece of the $\mathbf{p}$ integration then behaves as $\int_{\mathbf{p}}\mathbf{p}\cdot\mathbf{l}/p^4$, which is logarithmically UV divergent (from the point of view of absolute convergence). This can be remedied by rewriting the *regulated* version of Eq. (2.4) by using the freedom to change the integration variable $\mathbf{p}$ to $-\mathbf{p}$:

$$\Delta\langle\phi^2\rangle_{\mathrm{LO}}=-\int_{\mathbf{lp}}\frac{F_p}{l^4}\left[\frac{1}{2|\mathbf{l}+\mathbf{p}|^2}+\frac{1}{2|\mathbf{l}-\mathbf{p}|^2}-\frac{1}{p^2}\right]. \tag{2.5}$$

Now, if we throw away the UV regulator, the $\mathbf{l}$ fixed, large p divergence is gone. This sort of divergence is trivial, easy to remedy, and will not have much practical impact on our calculations (given the order in which we will eventually do integrations). We will simply acknowledge the issue in later calculations, without emphasizing it, by writing Eq. (2.5) as

$$\Delta\langle\phi^2\rangle_{\mathrm{LO}}=-\int_{\mathbf{lp}}\frac{F_p}{l^4}\left[\frac{1}{|\mathbf{l}+\mathbf{p}|^2}-\frac{1}{p^2}\right]_{\pm}, \tag{2.6}$$

where the subscript $\pm$ means that one should average the expression with $\mathbf{p}\to-\mathbf{p}$ (or equivalently with $\mathbf{l}\to-\mathbf{l}$).

Unfortunately, even Eq. (2.5) is not absolutely convergent. There is still a logarithmic UV divergence associated with $\mathbf{l}$ and $\mathbf{p}$ *simultaneously* becoming large ($l\sim p\to\infty$), as can be seen by simple power counting and the fact that F_p approaches a nonzero constant for large p. Return to considering Eq. (2.5) with a UV regulator still in place. We can eliminate the UV divergence by rewriting

$$\Delta\langle\phi^2\rangle_{\mathrm{LO}}=-\int_{\mathbf{lp}}\frac{(F_p-F_\infty)}{l^4}\left[\frac{1}{|\mathbf{l}+\mathbf{p}|^2}-\frac{1}{p^2}\right]_{\pm}-\int_{\mathbf{lp}}\frac{F_\infty}{l^4}\left[\frac{1}{|\mathbf{l}+\mathbf{p}|^2}-\frac{1}{p^2}\right]_{\pm}. \tag{2.7}$$

The second integral vanishes, as can be seen by changing the integration variable $\mathbf{p}\to\mathbf{p}-\mathbf{l}$ in its first term. So

$$\Delta\langle\phi^2\rangle_{\mathrm{LO}}=-\int_{\mathbf{lp}}\frac{(F_p-F_\infty)}{l^4}\left[\frac{1}{|\mathbf{l}+\mathbf{p}|^2}-\frac{1}{p^2}\right]_{\pm}. \tag{2.8}$$

This is now UV convergent because $F_p-F_\infty\to0$ as $p\to\infty$. However, we have traded the logarithmic UV divergence for a logarithmic infrared (IR) divergence, associated with $p\sim l\to0$.

We now need some sort of infrared regulator. One physically motivated possibility for consistently regulating the infrared would be to consider the system infinitesimally above the critical temperature, so that all the massless scalar propagators $1/p^2$ should be replaced by massive ones $1/(p^2+M^2)$, where M^2 represents a tiny, nonzero, inverse susceptibility χ^{-1}. This replacement defines an absolutely convergent integral in three dimensions, and the limit $M\to0$ would be taken only after the integrations.

Massless propagators $1/p^2$ will be much easier to deal with, however, in higher-order calculations. As a practical matter for computing diagrams, we prefer to introduce as few massive propagators as possible. It would be convenient, for example, to IR regulate Eq. (2.8) by introducing M only in the $1/l^2$ propagators:

$$\Delta\langle\phi^2\rangle_{\mathrm{LO}}=-\lim_{M\to0}\int_{\mathbf{lp}}\frac{(F_p-F_\infty)}{(l^2+M^2)^2}\left[\frac{1}{|\mathbf{l}+\mathbf{p}|^2}-\frac{1}{p^2}\right]_{\pm}, \tag{2.9}$$

where F_p is still defined in terms of the massless bubble integral, as in Eq. (2.2). One might worry that an *ad hoc* procedure of putting masses only on some propagators could be inconsistent, so let us argue more carefully. Return to the UV regulated version of Eq. (2.5) and note that the integral is not sensitive to the region of integration where l is infinitesimal, because this particular integral is IR convergent. There is then no reason we cannot modify the infrared behavior of the integrand for infinitesimal l, without affecting the integral. So, for instance,

$$\Delta\langle\phi^2\rangle_{\mathrm{LO}}=-\lim_{M\to0}\int_{\mathbf{lp}}\frac{F_p}{(l^2+M^2)^2}\left[\frac{1}{|\mathbf{l}+\mathbf{p}|^2}-\frac{1}{p^2}\right]_{\pm}. \tag{2.10}$$

But now, again rewriting $F_p=(F_p-F_\infty)+F_\infty$, the same steps as before reproduce Eq. (2.9).

Now that we have an absolutely convergent integral (2.9), we can do the integration in three dimensions and in any order we choose. It is convenient to do the $\mathbf{l}$ integral first:

$$\int_{\mathbf{l}}\frac{1}{(l^2+M^2)^2}\left[\frac{1}{|\mathbf{l}+\mathbf{p}|^2}-\frac{1}{p^2}\right]_{\pm}=\frac{1}{8\pi M(p^2+M^2)}-\frac{1}{8\pi Mp^2}=-\frac{M}{8\pi p^2(p^2+M^2)}. \tag{2.11}$$

The "$\pm$" prescription makes no difference to this particular integral, because the $\mathbf{l}$ integration by itself is completely convergent without it. Note that naively setting M to zero at this stage would give the incorrect, zero result mentioned earlier. Instead, we have

$$\Delta\langle\phi^2\rangle_{\mathrm{LO}}=\lim_{M\to0}\int_{\mathbf{p}}(F_p-F_\infty)\frac{M}{8\pi p^2(p^2+M^2)}. \tag{2.12}$$

The overall factor of M in the numerator is canceled by a linear IR divergence in the **p** integration, which is cut off by M.

For small M, the integral (2.12) is dominated[5] by $p \sim M$. So, in the limit of $M \to 0$, we can simplify the calculation slightly by replacing $F_p - F_\infty$ by $F_0 - F_\infty$. So

$$\Delta\langle\phi^2\rangle_{\rm LO} = (F_0 - F_\infty)\int_{\mathbf p} \frac{M}{8\pi p^2(p^2+M^2)} = \frac{F_0 - F_\infty}{32\pi^2}$$

$$= -\frac{Nu}{96\pi^2}. \qquad (2.13)$$

When combined with the formula (1.17) for ΔT_c, this reproduces Baym *et al.*'s leading large-N result (1.1), in which N has been set to 2.

III. NEXT ORDER IN 1/*N*

The diagrams which contribute to $\Delta\langle\phi^2\rangle$ at next order in $1/N$ are shown in Figs. 4 and 5. The diagrammatic expansion comes from the standard introduction of an auxiliary field σ, represented by the dashed lines.[6] The $O(N)$ action of Eq. (1.8) is rewritten as

$$S = \int d^3x \left[\frac{1}{2}|\Delta\phi|^2 + \frac{1}{2}r\phi^2 + \frac{1}{2}\phi^2\sigma - \frac{1}{6u}\sigma^2\right]. \qquad (3.1)$$

The σ propagator is then turned into the bubble chain of Fig. 2 by resumming the basic massless bubble of Fig. 6 into the σ propagator. Technically, this is accomplished by trivially rewriting Eq. (3.1) as

$$S = S_0 + S_{\rm subtractions} + \int d^3x \tfrac{1}{2}\phi^2\sigma, \qquad (3.2a)$$

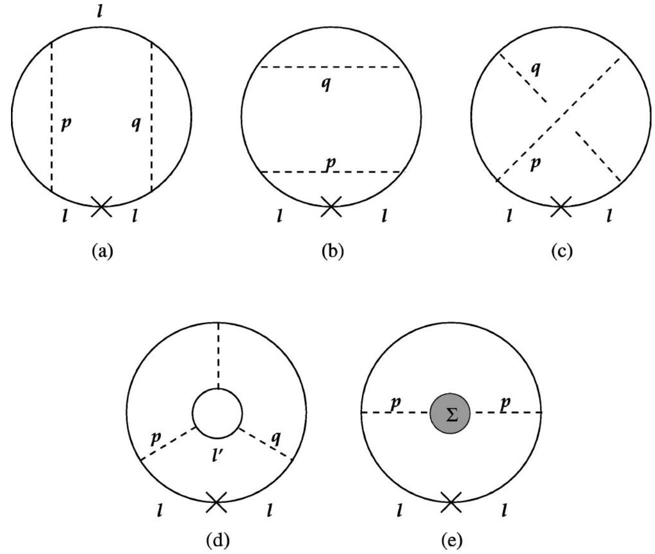

FIG. 4. Next-to-leading order diagrams for $\Delta\langle\phi^2\rangle$. $\mathbf{p},\mathbf{q},\mathbf{l},\mathbf{l}'$ label loop momenta, as used in the main text.

$$S_0 = \int_{\mathbf p} [\tfrac{1}{2}\phi_{-\mathbf p}p^2\phi_{\mathbf p} + \tfrac{1}{2}\sigma_{-\mathbf p}(-NF_{\mathbf p}^{-1})\sigma_{\mathbf p}], \qquad (3.2b)$$

$$S_{\rm subtractions} = \int_{\mathbf p} [\tfrac{1}{2}r\phi_{-\mathbf p}\phi_{\mathbf p} + \tfrac{1}{2}\sigma_{-\mathbf p}N\tilde\Sigma_0(p)\sigma_{\mathbf p}], \qquad (3.2c)$$

with F_p and $\tilde\Sigma_0$ given by Eq. (2.2). The terms designated $S_{\rm subtractions}$ may be ignored if one follows the previous *Rule 1* as well as the following.

Rule 2. Do not include any diagrams that have the one-loop bubble, Fig. 6, as a subdiagram.

Note that *Rule 1* eliminates any tadpole subdiagrams, such as Fig. 7. Formal large-N counting of diagrams is simply to count a factor of N^{-1} for each σ propagator and a factor of N for each ϕ loop. The important momentum scale of the problem will be the scale $p \sim Nu = O(N^0)$, where the σ propagator (2.1) makes the transition from its small-p behavior ($F_p \propto p$) to its large-p behavior ($F_p \to$const). Some authors like to completely integrate ϕ out of Eq. (3.1), but we prefer to retain it, as there is then a more transparent relationship between Feynman diagrams and the corresponding Feynman integrals.

In evaluating the diagrams of Fig. 4, we shall borrow techniques from Ref. [17], where somewhat related diagrams were evaluated in gauge theories with large numbers of scalars. Our strategy will be to do the ϕ loop integrals first, and then tackle the remaining integrals associated with σ propagators.

A. Diagram *a*

Let us start with Fig. 4(a). The corresponding integral is

---

[5]Some readers may worry that the integral (2.12) is dominated by arbitrarily small $p \sim M \to 0$. They may worry because at sufficiently small momentum our perturbative propagators are no longer good approximations to the full propagators. The *full* scalar propagators, for example, actually scale like $1/l^{2+\eta}$ rather than $1/l^2$ at small l ($\ll Nu$), where the critical exponent η is $O(N^{-1})$. The difference becomes significant when $l \lesssim Nu\,\exp(-\eta) = Nu\,\exp[-O(1/N)]$. One might worry that the sensitivity of Eq. (2.12) to $p \to 0$ is a sign that naive large-N perturbation theory must break down. It is important to realize, in the present case, that this infrared sensitivity is simply an artifact of our mathematical manipulations on the infrared-safe expression (2.9). Regardless of whether one used some sort of infrared-improved propagator in Eq. (2.9), that expression is not sensitive to far-infrared momenta. It is sensitive to momenta $\gtrsim Nu$, for which there is nothing wrong with a large-N expansion based on perturbative propagators.

[6]For a very quick review of standard large N, see, for example, section 2.1 of chapter 8 of [16]. Some people might prefer to replace σ by $i\sigma$ in the action (3.1), so that the imaginary-time path integral for σ is convergent, but it matters not at all for the purpose of large N perturbation theory.

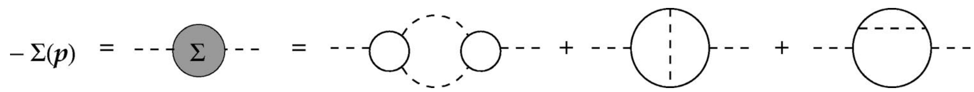

FIG. 5. Diagrams for the σ self-energy $\Sigma(p)$ at $O(N^0)$.

$$\Delta\langle\phi^2\rangle_{\rm a}=N^{-1}\int_{\mathbf{pq}}F_pF_q\int_{\mathbf{l}}\frac{1}{l^6}\left[\frac{1}{|\mathbf{l}+\mathbf{p}|^2}-\frac{1}{p^2}\right]_{\pm}\times\left[\frac{1}{|\mathbf{l}+\mathbf{q}|^2}-\frac{1}{q^2}\right]_{\pm}. \tag{3.3}$$

As written, this integral is absolutely convergent and can be evaluated, without regularization, directly in three dimensions. To do the $\mathbf{l}$ integration, however, we find it convenient to temporarily introduce an IR regulator mass M. We may then separately integrate each of the terms of the integrand, which are not individually IR convergent. We can also use M as a trick for reducing powers of l^{-2}. Specifically, we rewrite the $\mathbf{l}$ integral as the $M\to 0$ limit of

$$\int_{\mathbf{l}}\frac{1}{(l^2+M^2)^3}\left[\frac{1}{|\mathbf{l}+\mathbf{p}|^2}-\frac{1}{p^2}\right]_{\pm}\left[\frac{1}{|\mathbf{l}+\mathbf{q}|^2}-\frac{1}{q^2}\right]_{\pm}$$
$$=\frac{1}{2}\frac{d^2}{d(M^2)^2}\int_{\mathbf{l}}\frac{1}{(l^2+M^2)}\left[\frac{1}{|\mathbf{l}+\mathbf{p}|^2}-\frac{1}{p^2}\right]_{\pm}\left[\frac{1}{|\mathbf{l}+\mathbf{q}|^2}-\frac{1}{q^2}\right]_{\pm}$$
$$=\frac{1}{2}\frac{d^2}{d(M^2)^2}\Bigg[I_1(\mathbf{p},\mathbf{q};M)-p^{-2}J_1(\mathbf{q};M)-q^{-2}J_1(\mathbf{p};M)+p^{-2}q^{-2}\left(-\frac{M}{4\pi}\right)\Bigg]_{\pm}, \tag{3.4}$$

where

$$I_1(\mathbf{p},\mathbf{q};M)\equiv\int_{\mathbf{l}}\frac{1}{(l^2+M^2)|\mathbf{l}+\mathbf{p}|^2|\mathbf{l}+\mathbf{q}|^2}, \tag{3.5}$$

$$J_1(\mathbf{p};M)\equiv\int_{\mathbf{l}}\frac{1}{(l^2+M^2)|\mathbf{l}+\mathbf{p}|^2}, \tag{3.6}$$

and[7]

$$\int_{\mathbf{l}}\frac{1}{(l^2+M^2)^3}=\frac{1}{2}\frac{d^2}{d(M^2)^2}\int_{\mathbf{l}}\frac{1}{l^2+M^2}=\frac{1}{2}\frac{d^2}{d(M^2)^2}\left(-\frac{M}{4\pi}\right). \tag{3.7}$$

The integral J_1 is straightforward to evaluate. A particularly simple way to evaluate I_1 is to make a conformal transformation which reduces it to the form of J_1. The results of both integrals, and the conformal transformation between them, are discussed in the Appendix. All we need here are the small-M expansions of those results, which turn out to be

$$I_1(\mathbf{p},\mathbf{q};M)=\frac{1}{8pq|\mathbf{p}-\mathbf{q}|}-\frac{M}{4\pi p^2q^2}-\frac{M^2\mathbf{p}\cdot\mathbf{q}}{8p^3q^3|\mathbf{p}-\mathbf{q}|}+\frac{M^3(p^2+4\mathbf{p}\cdot\mathbf{q}+q^2)}{12\pi p^4q^4}+\frac{M^4[3(\mathbf{p}\cdot\mathbf{q})^2-p^2q^2]}{16p^5q^5|\mathbf{p}-\mathbf{q}|}+O(M^5), \tag{3.8}$$

$$J_1(\mathbf{p};M)=\frac{1}{8p}-\frac{M}{4\pi p^2}+\frac{M^3}{12\pi p^4}+O(M^5). \tag{3.9}$$

Putting everything together,

$$\int_{\mathbf{l}}\frac{1}{(l^2+M^2)^3}\left[\frac{1}{|\mathbf{l}+\mathbf{p}|^2}-\frac{1}{p^2}\right]_{\pm}\left[\frac{1}{|\mathbf{l}+\mathbf{q}|^2}-\frac{1}{q^2}\right]_{\pm}$$
$$=\left[\frac{\hat{\mathbf{p}}\cdot\hat{\mathbf{q}}}{8\pi Mp^3q^3}+\frac{3(\hat{\mathbf{p}}\cdot\hat{\mathbf{q}})^2-1}{16p^3q^3|\mathbf{p}-\mathbf{q}|}\right]_{\pm}+O(M)$$
$$=\left[\frac{3(\hat{\mathbf{p}}\cdot\hat{\mathbf{q}})^2-1}{16p^3q^3|\mathbf{p}-\mathbf{q}|}\right]_{\pm}+O(M). \tag{3.10}$$

We can now set $M=0$. All that will matter in the integral (3.3) is the average $\langle\ \rangle_\theta$ over the angle between $\mathbf{p}$ and $\mathbf{q}$, which is

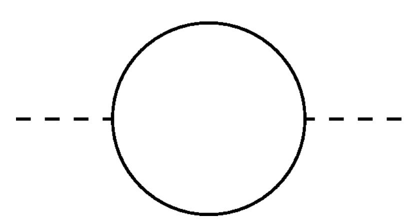

FIG. 6. The one-loop bubble diagram.

[7]The integral $\int_{\mathbf{l}}(l^2+M^2)^{-1}$ is $-M/4\pi$ plus an M-independent UV divergence, and M^2 derivatives of the latter vanish. It is of course not necessary to introduce $\int_{\mathbf{l}}(l^2+M^2)^{-1}$ and this spurious UV divergence; one could simply evaluate $\int_{\mathbf{l}}(l^2+M^2)^{-3}$ directly. But we find it convenient to consolidate the treatment of such integrals with that of the other terms in Eq. (3.4).

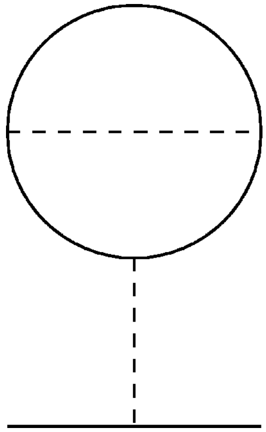

FIG. 7. Example of a tadpole diagram.

$$\left\langle \int_{\mathbf{l}} \frac{1}{l^6}\left[\frac{1}{|\mathbf{l}+\mathbf{p}|^2}-\frac{1}{p^2}\right]_{\pm}\left[\frac{1}{|\mathbf{l}+\mathbf{q}|^2}-\frac{1}{q^2}\right]_{\pm}\right\rangle_{\theta}=\frac{1}{40p_>^6 p_<}, \tag{3.11}$$

where

$$p_> \equiv \max(p,q), \quad p_< \equiv \min(p,q). \tag{3.12}$$

We are left with

$$\Delta\langle\phi^2\rangle_a=\frac{1}{N}\int_{\mathbf{pq}}\frac{F_pF_q}{40p_>^6p_<}=\frac{1}{2\pi^4N}\int_0^\infty p^2dp\int_0^p q^2dq\,\frac{F_pF_q}{40p^6q}. \tag{3.13}$$

The remaining integrals are easy to do, with the result

$$\Delta\langle\phi^2\rangle_{\mathrm{a}}=\frac{u}{15\pi^4}\left(\frac{\pi^2}{6}-\frac{5}{4}\right). \tag{3.14}$$

B. Diagram *b*

Figure 4(b) corresponds to

$$\Delta\langle\phi^2\rangle_{\mathrm{b}}=N^{-1}\int_{\mathbf{pq}}F_pF_qB_{\mathbf{pq}}, \tag{3.15a}$$

$$B_{\mathbf{pq}}\equiv\int_{\mathbf{l}}\frac{1}{l^4}\left\{\frac{1}{|\mathbf{l}+\mathbf{p}|^4}\left[\frac{1}{|\mathbf{l}+\mathbf{p}+\mathbf{q}|^2}-\frac{1}{q^2}\right]-\frac{1}{p^4}\left[\frac{1}{|\mathbf{p}+\mathbf{q}|^2}-\frac{1}{q^2}\right]\right\}_{\pm}. \tag{3.15b}$$

This contribution to $\Delta\langle\phi^2\rangle$ is again absolutely convergent if the subscript $\pm$ is taken to mean averaging over $\mathbf{p}\to-\mathbf{p}$ and also over $\mathbf{q}\to-\mathbf{q}$. It is convenient now to rewrite the $\mathbf{l}$ integral as the $M_1,M_2\to 0$ limit of

$$\begin{aligned}&\int_{\mathbf{l}}\frac{1}{(l^2+M_1^2)^2}\left\{\frac{1}{(|\mathbf{l}+\mathbf{p}|^2+M_2^2)^2}\left[\frac{1}{|\mathbf{l}+\mathbf{p}+\mathbf{q}|^2}-\frac{1}{q^2}\right]-\frac{1}{(p^2+M_2^2)^2}\left[\frac{1}{|\mathbf{p}+\mathbf{q}|^2}-\frac{1}{q^2}\right]\right\}_{\pm}\\&=\frac{d}{d(M_1^2)}\frac{d}{d(M_2^2)}\left\{I_2(\mathbf{p}+\mathbf{q},\mathbf{q},M_1,M_2)-\frac{1}{q^2}J_2(\mathbf{p};M_1,M_2)-\frac{1}{(p^2+M_2^2)}\left[\frac{1}{|\mathbf{p}+\mathbf{q}|^2}-\frac{1}{q^2}\right]\left(-\frac{M_1}{4\pi}\right)\right\}_{\pm},\end{aligned} \tag{3.16}$$

where

$$I_2(\mathbf{p},\mathbf{q};M_1,M_2)\equiv\int_{\mathbf{l}}\frac{1}{l^2(|\mathbf{l}+\mathbf{p}|^2+M_1^2)(|\mathbf{l}+\mathbf{q}|^2+M_2^2)}, \tag{3.17}$$

$$J_2(\mathbf{p};M_1,M_2)\equiv\int_{\mathbf{l}}\frac{1}{(l^2+M_1^2)(|\mathbf{l}+\mathbf{p}|^2+M_2^2)}. \tag{3.18}$$

The results for I_2 and J_2, and their small M_1,M_2 expansions, are given in the Appendix. The final result for the $\mathbf{l}$ integration, after taking the $M_1,M_2\to 0$ limit, is

$$B_{\mathbf{pq}}=\left[\frac{q-2p(\hat{\mathbf{p}}\cdot\hat{\mathbf{q}})-3q(\hat{\mathbf{p}}\cdot\hat{\mathbf{q}})^2}{8p^3q^2|\mathbf{p}+\mathbf{q}|^3}\right]_{\pm}, \tag{3.19}$$

with angular average

$$\langle B_{\mathbf{pq}}\rangle_\theta=\frac{\theta(p-q)}{4p^6q}, \tag{3.20}$$

where $\theta(p-q)$ is the step function (1 for $p>q$; 0 for $p<q$). The remaining integrals are easy to do, giving

$$\Delta\langle\phi^2\rangle_{\mathrm{b}}=\frac{u}{3\pi^4}\left(\frac{\pi^2}{6}-\frac{5}{4}\right). \tag{3.21}$$

C. Diagram *c*

Figure 4(c) can be evaluated as the others, but the final integrals are a bit more complex. The diagram gives

$$\Delta\langle\phi^2\rangle_{\mathrm{c}}=N^{-1}\int_{\mathbf{pq}}F_pF_qC_{\mathbf{pq}}, \tag{3.22a}$$

$$C_{\mathbf{pq}}\equiv\int_{\mathbf{l}}\frac{1}{l^4}\left[\frac{1}{|\mathbf{l}+\mathbf{p}|^2|\mathbf{l}+\mathbf{q}|^2|\mathbf{l}+\mathbf{p}+\mathbf{q}|^2}-\frac{1}{p^2q^2|\mathbf{p}+\mathbf{q}|^2}\right]_{\pm}. \tag{3.22b}$$

The **l** integration can be performed using methods similar to before:

$$C_{\mathbf{pq}} = -\lim_{M\to 0}\frac{d}{d(M^2)}\left[H(\mathbf{p},\mathbf{q};M) - \frac{1}{p^2q^2|\mathbf{p}+\mathbf{q}|^2}\left(-\frac{M}{4\pi}\right)\right]_{\pm}, \tag{3.23}$$

$$H(\mathbf{p},\mathbf{q};M) \equiv \int_{\mathbf{l}} \frac{1}{(l^2+M^2)|\mathbf{l}+\mathbf{p}|^2|\mathbf{l}+\mathbf{q}|^2|\mathbf{l}+\mathbf{p}+\mathbf{q}|^2}. \tag{3.24}$$

H can be reduced to the basic integrals I_1 and J_1 encountered previously by rewriting the numerator 1 in Eq. (3.24) as

$$1 = \frac{1}{2\mathbf{p}\cdot\mathbf{q}+M^2}[(l^2+M^2)+|\mathbf{l}+\mathbf{p}+\mathbf{q}|^2-|\mathbf{l}+\mathbf{p}|^2-|\mathbf{l}+\mathbf{q}|^2] \tag{3.25}$$

and then expanding the integrand into the corresponding four terms:

$$H(\mathbf{p},\mathbf{q};M) = \frac{1}{2\mathbf{p}\cdot\mathbf{q}+M^2}[I_1(\mathbf{p},\mathbf{q};0)+I_1(\mathbf{p},\mathbf{q};M) - I_1(\mathbf{p}+\mathbf{q},\mathbf{q};M)-I_1(\mathbf{p}+\mathbf{q},\mathbf{p};M)]. \tag{3.26}$$

Using the expansion (3.8) of I_1, one obtains

$$C_{\mathbf{pq}} = \left[\frac{1}{16p^3q^3}[1+(\hat{\mathbf{p}}\cdot\hat{\mathbf{q}})^{-2}]\left(\frac{1}{|\mathbf{p}-\mathbf{q}|}-\frac{1}{|\mathbf{p}+\mathbf{q}|}\right) + \frac{\hat{\mathbf{p}}\cdot\hat{\mathbf{q}}-(\hat{\mathbf{p}}\cdot\hat{\mathbf{q}})^{-1}}{8p^2q^2|\mathbf{p}+\mathbf{q}|^3}\right]_{\pm}. \tag{3.27}$$

This simplifies, after applying the $[\cdots]_{\pm}$ prescription, to

$$C_{\mathbf{pq}} = \frac{\hat{\mathbf{p}}\cdot\hat{\mathbf{q}}-(\hat{\mathbf{p}}\cdot\hat{\mathbf{q}})^{-1}}{16p^2q^2}\left[\frac{1}{|\mathbf{p}+\mathbf{q}|^3}-\frac{1}{|\mathbf{p}-\mathbf{q}|^3}\right]. \tag{3.28}$$

Angular averaging yields

$$\langle C_{\mathbf{pq}}\rangle_\theta = \frac{1}{8p_>^7x^2(1+x^2)}\left[x+\frac{\mathrm{Sinh}^{-1}x}{\sqrt{1+x^2}}\right], \tag{3.29}$$

where

$$x \equiv p_</p_>. \tag{3.30}$$

The remaining integrals over **p** and **q** are no longer so trivial. Notice first that for an arbitrary function $f(x)$ one can rewrite

$$\frac{1}{N}\int_{\mathbf{pq}}\frac{F_pF_q}{p_>^7}f(x) = \frac{1}{2\pi^4N}\int_0^\infty dp\int_0^1 dx\,\frac{F_pF_{xp}}{p^2}x^2f(x) = -\frac{8u}{3\pi^4}\int_0^1 dx\,\frac{x^3\ln x}{(1-x)}f(x), \tag{3.31}$$

so that

$$\Delta\langle\phi^2\rangle_c = -\frac{u}{3\pi^4}\int_0^1 dx\frac{x\ln x}{(1-x)}\left[\frac{x}{1+x^2}+\frac{\mathrm{Sinh}^{-1}x}{(1+x^2)^{3/2}}\right]. \tag{3.32}$$

This is easiest to evaluate numerically, giving

$$\Delta\langle\phi^2\rangle_c = \frac{cu}{3\pi^4}, \tag{3.33}$$

where $c \simeq 0.463\,715$. We also have an analytic result:[8]

$$c = \frac{\pi^2}{48}\left[1+\frac{7}{\sqrt{2}}\ln(1+\sqrt{2})\right]-\frac{2}{3}L(3,\chi_8), \tag{3.34}$$

where

$$L(s,\chi_8) = 1-\frac{1}{3^s}-\frac{1}{5^s}+\frac{1}{7^s}+\frac{1}{9^s}-\frac{1}{11^s}-\frac{1}{13^s}+\frac{1}{15^s}+\frac{1}{17^s}-\ \ldots \tag{3.35a}$$

is a particular case of Dirichlet's L function, and

$$L(3,\chi_8) = 0.958\,380\,454\,563\ldots. \tag{3.35b}$$

D. Diagram *d*

Figure 4(d) corresponds to

$$\Delta\langle\phi^2\rangle_d = -N^{-1}\int_{\mathbf{pq}}F_pF_qF_{|\mathbf{q}-\mathbf{p}|}D_{\mathbf{pq}}, \tag{3.36a}$$

[8]Our inelegant, brute force method for obtaining this result is borrowed from a footnote of Ref. [17]. The hard part is the Sinh^{-1} term. We change variables from x to $y=x+\sqrt{1+x^2}$. This turns $\mathrm{Sinh}^{-1}x$ into $\ln y$. $\ln x$ can be written as a sum of terms of the form $\ln(y-a)$, and the change of integration variable makes the rest of the integrand a rational function of y. We then split this rational function apart by partial fractions and do each integral, yielding dilogarithms and trilogarithms of various arguments. Finally, we use a zoo of polylogarithm identities [18] to simplify the answer.

$$D_{\mathbf{pq}} \equiv \int_{\mathbf{l}'} \frac{1}{l'^2|\mathbf{l}'+\mathbf{p}|^2|\mathbf{l}'+\mathbf{q}|^2}\int_{\mathbf{l}} \frac{1}{l^4}\left[\frac{1}{|\mathbf{l}+\mathbf{p}|^2|\mathbf{l}+\mathbf{q}|^2}-\frac{1}{p^2q^2}\right]_{\pm\mathbf{l}}$$

$$= -I_1(\mathbf{p},\mathbf{q};0)\lim_{M\to 0}\frac{d}{d(M^2)}\left[I_1(\mathbf{p},\mathbf{q},M) - p^{-2}q^{-2}\left(-\frac{M}{4\pi}\right)\right]$$

$$= \frac{\hat{\mathbf{p}}\cdot\hat{\mathbf{q}}}{64p^3q^3|\mathbf{p}-\mathbf{q}|^2}. \tag{3.36b}$$

Here the subscript $\pm\mathbf{l}$ means we implicitly average over $\mathbf{l}\to-\mathbf{l}$ for absolute convergence. Doing the remaining integrals by brute force, we find

$$\Delta\langle\phi^2\rangle_{\rm d} = \frac{u}{\pi^4}\left[\frac{7}{12}\left(\zeta(3)-\frac{\pi^2}{6}\right)+\frac{1}{6}\right], \tag{3.37}$$

where ζ is the Riemann zeta function. It is interesting to note that $\pi^2/6$ can also be written as $\zeta(2)$.

E. Diagram *e*

The final class of diagrams, Fig. 4(e), corresponds to the leading-order diagram, Fig. 1, with the replacement

$$-N^{-1}F_{\mathbf{p}} \to (-N^{-1}F_{\mathbf{p}})[-\Sigma(p)](-N^{-1}F_{\mathbf{p}}) \equiv -N^{-1}\mathcal{F}_{\mathbf{p}}, \tag{3.38}$$

where $\Sigma(p)$ represents the contribution to the σ self-energy at next-to-leading order, shown in the diagrams of Fig. 5. Making this substitution in the leading-order calculation (2.13) gives

$$\Delta\langle\phi^2\rangle_{\rm e} = \frac{\mathcal{F}_0-\mathcal{F}_\infty}{32\pi^2}. \tag{3.39}$$

The nice feature of this relation is that we only need to calculate $\Sigma(p)$ in the small and large p limits.

The first self-energy diagram in Fig. 5 contributes,

$$\Sigma_1(\mathbf{p}) = -\tfrac{1}{2}\int_{\mathbf{q}} F_q F_{|\mathbf{p}+\mathbf{q}|}\int_{\mathbf{l}_1}\frac{1}{l_1^2|\mathbf{l}_1+\mathbf{p}|^2|\mathbf{l}_1+\mathbf{p}+\mathbf{q}|^2} \times \int_{\mathbf{l}_2}\frac{1}{l_2^2|\mathbf{l}_2+\mathbf{p}|^2|\mathbf{l}_2+\mathbf{p}+\mathbf{q}|^2}. \tag{3.40}$$

For small $\mathbf{p}$, the integration is dominated by $l_1, l_2 \sim p$, and $q\sim Nu$. So we can ignore $\mathbf{l}_1$, $\mathbf{l}_2$, and $\mathbf{p}$ compared to $\mathbf{q}$ and write[9]

$$\Sigma_1(\mathbf{p}) \to -\tfrac{1}{2}\int_{\mathbf{q}} q^{-4}F_q^2\left[\int_{\mathbf{l}}\frac{1}{l^2|\mathbf{l}+\mathbf{p}|^2}\right]^2 = -\frac{Nu}{48\pi^2p^2}. \tag{3.41}$$

This diagram has a quadratic IR divergence for $\mathbf{p}=0$. In contrast, the other two diagrams only diverge as linear×log when $\mathbf{p}=0$, and so behave as $p^{-1}\ln p$ for small p. In summary,

$$\Sigma(\mathbf{p}) = -\frac{Nu}{48\pi^2p^2} + O(p^{-1}\ln p) \tag{3.42}$$

for small $\mathbf{p}$. One may check by power counting diagrams and subdiagrams that $\Sigma(\infty)=0$. Then

$$\mathcal{F}_0 = -\frac{16}{3\pi^2}u, \quad \mathcal{F}_\infty = 0, \tag{3.43}$$

and

$$\Delta\langle\phi^2\rangle_{\rm e} = -\frac{u}{6\pi^4}. \tag{3.44}$$

One may also check this answer by direct, brute-force calculation of all the diagrams associated with Fig. 4(e).

We conclude by mentioning one technical subtlety, glossed over above, concerning absolute convergence. The integration corresponding to the substitution (3.38) in the leading-order analysis is

$$\Delta\langle\phi^2\rangle_{\rm e} = -\int_{\mathbf{lp}}\frac{\mathcal{F}_p}{l^4}\left[\frac{1}{|\mathbf{l}+\mathbf{p}|^2}-\frac{1}{p^2}\right]_{\pm}. \tag{3.45}$$

In contrast to the analogous leading-order expression (2.6), this integral is not absolutely convergent in the infrared ($l\sim p\to 0$), though it is convergent in the UV. One might therefore worry about the *ad hoc* introduction of an IR regulator M in the calculation of this graph. However, this worry is easily bypassed by rewriting

$$\Delta\langle\phi^2\rangle_{\rm e} = -\int_{\mathbf{lp}}\frac{(\mathcal{F}_p-\mathcal{F}_0)}{l^4}\left[\frac{1}{|\mathbf{l}+\mathbf{p}|^2}-\frac{1}{p^2}\right]_{\pm}, \tag{3.46}$$

which should be understood as regulated in the UV. The UV-regulated integral of the $\mathcal{F}_0$ factor vanishes. Equation (3.46) is now convergent in the IR, but logarithmically divergent in the UV, just as the original leading-order integral (2.6) was. One can now follow through the same argument as in the leading-order case to introduce an IR regulator and then remove the UV divergence, where F_p in the leading-order analysis is now replaced by $\mathcal{F}_p-\mathcal{F}_0$. The result is still Eq. (3.39).

[9]For general p, the result is $Nu\Sigma_1(p)=24\pi^{-2}z^{-3}{\rm Re}[2\,{\rm Li}_2(-z)-2\,{\rm Li}_2(2+z)+\frac{1}{2}\pi^2]$, where $z\equiv 48p/Nu$, and ${\rm Li}_2(z)\equiv -\int_0^z dx\,\ln(1-x)/x$ is the dilogarithm function. One may double check that the $p\to 0$ limit agrees with Eq. (3.41).

F. Summary

Summing all the diagrams then yields the total NLO contribution:

$$\Delta\langle\phi^2\rangle_{\rm NLO}=\frac{u}{3\pi^4}\left[\frac{7}{4}\zeta(3)-\frac{3}{2}-\frac{17}{240}\pi^2+\frac{7\pi^2}{48\sqrt{2}}\ln(1+\sqrt{2})-\frac{2}{3}L(3,\chi_8)\right], \tag{3.47}$$

with $L(3,\chi_8)$ given by Eq. (3.35). Combining with the leading-order result (2.13),

$$\frac{\Delta\langle\phi^2\rangle_{\rm NLO}}{\Delta\langle\phi^2\rangle_{\rm LO}}=-\frac{0.527\,198}{N}, \tag{3.48}$$

which is the relative NLO correction we presented for T_c in Eq. (1.4).

ACKNOWLEDGMENTS

We are indebted to Eric Braaten for suggesting this project. We are also grateful to Tim Newman and Genya Kolemeisky for useful discussions. This work was supported, in part, by the U.S. Department of Energy under Grant No. DE-FG02-97ER41027.

APPENDIX: BASIC INTEGRALS

Let us begin with the integral $J_2(\mathbf{p};M_1,M_2)$. This is quite easy to do by standard methods (for example, by introducing a Feynman parameter), and gives

$$J_2(\mathbf{p};M_1,M_2)\equiv\int_{\mathbf{l}}\frac{1}{(l^2+M_1^2)(|\mathbf{l}+\mathbf{p}|^2+M_2^2)}$$
$$=\frac{1}{8\pi p}\cos^{-1}\left(\frac{(M_1+M_2)^2-p^2}{(M_1+M_2)^2+p^2}\right)$$
$$=\frac{1}{8p}-\frac{(M_1+M_2)}{4\pi p^2}+\frac{(M_1+M_2)^3}{12\pi p^4}+O(M^5). \tag{A1}$$

The integral $J_1(\mathbf{p};m)$ of Eq. (3.6) is simply the special case $J_1(\mathbf{p};M)=J_2(\mathbf{p};M,0)$.

The integral $I_2(\mathbf{p},\mathbf{q};M_1,M_2)$ of Eq. (3.17) can be related to $J_2(\mathbf{p},\mathbf{q};M_1,M_2)$ by generalizing a trick presented in Ref. [17]. The idea is to change integration variables from $\mathbf{l}$ to its conformal inversion $\tilde{\mathbf{l}}\equiv\mathbf{l}/l^2$. The integration measure changes as $(2\pi)^{-3}d^3l=(2\pi)^{-3}\tilde{l}^{-6}d^3\tilde{l}$. Propagators can be written in terms of the new variable $\tilde{\mathbf{l}}$ as

$$\frac{1}{l^2}=\tilde{l}^{\,2}, \tag{A2}$$

$$\frac{1}{|\mathbf{l}+\mathbf{p}|^2+M^2}=\frac{\tilde{l}^{\,2}}{(p^2+m^2)[|\tilde{\mathbf{l}}+\tilde{\mathbf{P}}|^2+\tilde{M}_p^2]}, \tag{A3}$$

where

$$\tilde{\mathbf{P}}\equiv\frac{\mathbf{p}}{p^2+M^2},\qquad \tilde{M}_p\equiv\frac{M}{p^2+M^2}. \tag{A4}$$

Making this change of variables,

$$I_2(\mathbf{p},\mathbf{q};M_1,M_2)\equiv\frac{1}{(p^2+M_1^2)(q^2+M_2^2)}\int_{\tilde{l}}\left[\left|\tilde{\mathbf{l}}+\frac{\mathbf{p}}{p^2+M_1^2}\right|^2+\left(\frac{M_1}{p^2+M_1^2}\right)^2\right]^{-1}\left[\left|\tilde{\mathbf{l}}+\frac{\mathbf{q}}{q^2+M_2^2}\right|^2+\left(\frac{M_2}{q^2+M_2^2}\right)^2\right]^{-1}$$
$$=\frac{1}{(p^2+M_1^2)(q^2+M_2^2)}J_2\left[\frac{\mathbf{p}}{p^2+M_1^2}-\frac{\mathbf{q}}{q^2+M_2^2};\frac{M_1}{p^2+M_1^2},\frac{M_2}{q^2+M_2^2}\right]. \tag{A5}$$

For the application of this paper, the relevant terms in the small M_1,M_2 expansion of I_2 are

$$I_2(\mathbf{p},\mathbf{q};M_1,M_2)=\frac{1}{8pq|\mathbf{p}-\mathbf{q}|}-\frac{1}{4\pi|\mathbf{p}-\mathbf{q}|^2}\left(\frac{M_1}{p^2}+\frac{M_2}{q^2}\right)+O(M_1^2)+O(M_2^2)+\frac{M_1M_2}{4\pi|\mathbf{p}-\mathbf{q}|^4}\left(\frac{M_1}{q^2}+\frac{M_2}{p^2}\right)+O(M_1^4)$$
$$+O(M_2^4)+M_1^2M_2^2\frac{[3pq-2(p^2+q^2)(\hat{\mathbf{p}}\cdot\hat{\mathbf{q}})+pq(\hat{\mathbf{p}}\cdot\hat{\mathbf{q}})^2]}{8p^2q^2|\mathbf{p}-\mathbf{q}|^5}+O(M^5). \tag{A6}$$

The integral I_1 of Eq. (3.5) is related by $I_1(\mathbf{p},\mathbf{q};M)=I_2(\mathbf{p},\mathbf{p}-\mathbf{q};M,0)$ and gives

$$I_1(\mathbf{p},\mathbf{q};M) = \frac{\cos^{-1}(2\omega_{\mathbf{pq}}^2 - 1)}{8\pi M|\mathbf{p}-\mathbf{q}|^2\sqrt{\omega_{\mathbf{pq}}^{-2}-1}}, \tag{A7}$$

where

$$\omega_{\mathbf{pq}} \equiv \frac{M|\mathbf{p}-\mathbf{q}|}{\sqrt{(p^2+M^2)(q^2+M^2)}}. \tag{A8}$$

The small M expansion is given in Eq. (3.8).

[1] P. Grüter, D. Ceperley, and F. Laloë, Phys. Rev. Lett. **79**, 3549 (1997).

[2] M. Holzmann, P. Grüter, and F. Laloë, Eur. Phys. J. B **10**, 739 (1999).

[3] H.T.C. Stoof, Phys. Rev. A **45**, 8398 (1982); M. Bijlsma and H.T.C. Stoof, *ibid.* **54**, 5085 (1996).

[4] A.M.J. Schakel, Int. J. Mod. Phys. B **8**, 2021 (1994).

[5] G. Baym, J.-P. Blaizot, M. Holzmann, F. Laloë, and D. Vautherin, Phys. Rev. Lett. **83**, 1703 (1999).

[6] M. Holzmann and W. Krauth, Phys. Rev. Lett. **83**, 2687 (1999).

[7] G. Baym, J.-P. Blaizot, and J. Zinn-Justin, Europhys. Lett. **49**, 150 (2000).

[8] J. Reppy, B. Crooker, B. Hebral, A. Corwin, J. He, and G. Zassanhaus, Phys. Rev. Lett. **84**, 2060 (2000).

[9] Y. Okabe and M. Oku, Prog. Theor. Phys. **60**, 1287 (1978); I. Kondor and T. Temesvári, J. Phys. (France) Lett. **39**, L99 (1978); **39**, L415(E) (1978).

[10] M. Fisher, Phys. Rev. **176**, 257 (1968).

[11] J.C. Le Guillon and J. Zinn-Justin, Phys. Rev. B **21**, 3976 (1980); Phys. Rev. Lett. **39**, 95 (1977); G.A. Baker, B.G. Nickel, and D.I. Meiron, Phys. Rev. B **17**, 1365 (1978); G.A. Baker, B.G. Nickel, M.S. Green, and D.I. Meiron, Phys. Rev. Lett. **36**, 1351 (1976).

[12] F. Dalfovo, S. Giorgini, and L.P. Pitaevskii, Rev. Mod. Phys. **71**, 463 (1999).

[13] E. Braaten and A. Nieto, Phys. Rev. B **55**, 8090 (1997); Eur. Phys. J. B **11**, 143 (1999).

[14] T.D. Lee and C.N. Yang, Phys. Rev. **105**, 1119 (1957); T.D. Lee, K. Huang, and C.N. Yang, *ibid.* **106**, 1135 (1957); T.T. Wu, *ibid.* **115**, 1390 (1959); N.M. Hugenholtz and D. Pines, *ibid.* **116**, 489 (1959); K. Sawada, *ibid.* **116**, 1344 (1959).

[15] H. Hammer and R. Furnstahl, Nucl. Phys. A **678**, 277 (2000).

[16] S. Coleman, *Aspects of Symmetry* (Cambridge University Press, Cambridge, 1985).

[17] P. Arnold and D. Wright, Phys. Rev. D **55**, 6274 (1997).

[18] L. Lewin, *Polylogarithms and Associated Functions* (Elsevier, New York, 1981) [or see the older version: L. Lewin *Dilogarithms and Associated Functions* (MacDonald, London, 1958)]; *Structual Properties of Polylogarithms*, edited by L. Lewin, Mathematical Surveys and Monographs Vol. 37 (American Mathematical Society, Providence, 1991); D. Zagier, in *Arithmetic Algebraic Geometry*, edited by F. van der Greet *et al.* (Birkhäuser, Boston, 1991), pp. 391–430.